2 February 1996

ELSEVIER

Chemical Physics Letters 249 (1995) 210–217

CHEMICAL PHYSICS LETTERS

High-resolution multiple quantum MAS NMR spectroscopy of half-integer quadrupolar nuclei

Gang Wu [a,b], David Rovnyank [a,b], Boqin Sun [a,b], Robert G. Griffin [a,b,*]

[a] *Francis Bitter Magnet Laboratory, Massachusetts Institute of Technology, Cambridge, MA 02139, USA*
[b] *Department of Chemistry, Massachusetts Institute of Technology, Cambridge, MA 02139, USA*

Received 27 September 1995; in final form 21 November 1995

Abstract

We demonstrate the utility of a two-pulse sequence in obtaining high-resolution solid state NMR spectra of half-integer quadrupolar nuclei with magic-angle-spinning (MAS). The experiment, which utilizes multiple/single-quantum correlation, was first described in a different form by Frydman and Harwood [J. Am. Chem. Soc. 117 (1995) 5367] and yields high-resolution isotropic NMR spectra where shifts are determined by the sum of resonance offset (chemical shift) and second-order quadrupolar effects. The two-pulse sequence described here is shown to provide a higher and more uniform excitation of multiple-quantum coherence than the three-pulse sequence used previously.

1. Introduction

High-resolution solid-state NMR spectroscopy is used extensively for studying a great variety of solid materials ranging from ceramics to biopolymers. However, most successful applications have involved spin $I = 1/2$ nuclei such as ^{13}C, ^{15}N, ^{31}P, etc. The reason for this is the problem in recording high-resolution NMR spectra for $I > 1/2$ nuclei in the presence of large quadrupolar interactions. For half-integer quadrupolar nuclei such as $^{23}Na(I = 3/2)$, $^{27}Al(I = 5/2)$ and $^{17}O(I = 5/2)$, improved spectral resolution can be obtained by observing the central $(1/2, -1/2)$ transition that is not influenced by first-order quadrupolar interactions [1–3]. However, the spectra are broadened by second-order quadrupolar effects. Specifically, the second-order quadrupolar interaction is a fourth rank interaction that cannot be averaged to zero by the magic-angle-spinning (MAS) technique which is successful in averaging second rank couplings such as dipolar interactions and the chemical shift anisotropy. Several years ago, dynamic-angle spinning (DAS) [4,5] and double-rotation (DOR) [6–8] techniques were developed for obtaining high-resolution isotropic NMR spectra for half-integer quadrupolar nuclei. DAS experiments involve sequential sample rotation at two complementary angles, while DOR experiments require the sample being spun simultaneously at two angles. With these techniques, it is possible to average both second and fourth rank interactions and obtain solid-state NMR spectra for half-integer quadrupolar nuclei which exhibit a resolution similar to that observed from spin-1/2 nuclei. However, both types of experiments are technically demanding and require specially designed NMR probes.

* Corresponding author.

Elsevier Science B.V.
SSDI 0009-2614(95)01376-8

Recently, Frydman and Harwood [9] demonstrated the possibility of obtaining isotropic NMR spectra for half-integer quadrupolar nuclei by correlating the evolution of the multiple-quantum (MQ) coherence $(m, -m)$ with that of the central $(1/2, -1/2)$. Because the evolution of this particular multiple-quantum coherence is governed by a Hamiltonian similar to that under which the central $(1/2, -1/2)$ transition evolves, it is possible for the evolution of the coherence to be refocused after the transfer of the multiple-quantum coherence into the central transition. Since the technique involves sample rotation at the magic angle, it can be implemented easily using an ordinary MAS probe.

The sensitivity of this new type of experiments depends critically on efficient excitation of the multiple-quantum coherence. In contrast to situations in solution NMR studies where two radio-frequency (RF) pulses are necessary for generating multiple-quantum coherences, a single finite RF pulse is capable of exciting multiple-quantum coherences for half-integer quadrupolar nuclei in the solid state [10–15]. In this Letter, we demonstrate the utility of two-pulse sequence (Fig. 1b) in performing triple-quantum (3Q) MAS experiments. As an example, we present $^{17}O(I = 5/2)$ NMR results for ^{17}O-enriched hydroxyapatite ($Ca_5(P^{17}O_4)_3OH$) and $^{23}Na(I = 3/2)$ results for anhydrous $^{23}Na_2SO_4$ and $^{23}Na_2HPO_4$.

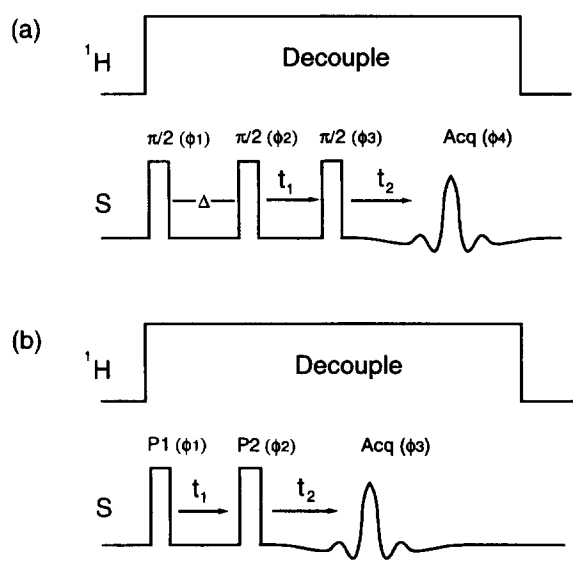

Fig. 1. RF pulse sequences for the 3Q-MAS experiment. (a) The basic three-pulse sequence, $P_1 = P_2 = P_3 = 90°$ [9]; (b) the two-pulse sequence used in this study.

2. Theoretical background

2.1. Removal of $l = 4$ terms in the effective Hamiltonian

Consider a spin system consisting of half-integer spin nuclei ($I > 1$) that are subjected to quadrupolar and chemical shielding interactions. In the rotating frame, the average Hamiltonian (to first order) can be written as [16]

$$H = H_{CS} + H_Q^{(0)} + H_Q^{(1)}, \tag{1}$$

where H_{CS} is the chemical shielding Hamiltonian, $H_Q^{(0)}$ and $H_Q^{(1)}$ are the zeroth- and first-order average Hamiltonians arising from the quadrupolar interaction and describe the first- and second-order quadrupolar interactions, respectively. In this Letter, we are only concerned with the $(m, -m)$ coherences where m is the magnetic quantum number; as the evolutions of such coherences are unaffected by the first-order quadrupolar interaction, $H_Q^{(0)}$ can be neglected. For ease of discussion, H_{CS} and $H_Q^{(1)}$ can be expressed according to the fictitious spin-1/2 operators [10,11] as

$$H_{CS} = \sum_{l=0,2} \sum_m 2mA_{l0}^{CS} I_z^{m,-m}, \tag{2}$$

$$H_Q^{(1)} = \sum_{l=0,2,4} \sum_m C_{lm} A_{l0}^{Q} I_z^{m,-m}, \tag{3}$$

where

$$C_{lm}(I) = \frac{\omega_Q^2}{\omega_0}\left[a_{m,-m}^{(1)} C(2, 2, l, 1, -1) + a_{m,-m}^{(2)} C(2, 2, l, 2, -2)\right] \tag{4}$$

and

$$a_{m,-m}^{(1)} = m\left[4I(I+1) - 8m^2 - 1\right], \tag{5}$$

$$a_{m,-m}^{(2)} = m\left[2I(I+1) - 2m^2 - 1\right]. \tag{6}$$

In Eq. (4), $C(2, 2, l, 1, -1)$ and $C(2, 2, l, 2, -2)$ are the Clebsch–Gordan coefficients. A_{l0}^{CS} and A_{l0}^{Q} describe the orientation dependence of the chemical shielding and quadrupolar interactions, respectively.

If the $(m, -m)$ coherence ($m \neq 1/2$) is allowed to evolve for a period of time, t_1, the propagator, $U(t_1, 0)$, can be written as

$$U(t_1, 0) = \exp(-iH_{m,-m}t_1). \quad (7)$$

If the $(m, -m)$ coherence is transferred into the central $(1/2, -1/2)$ transition and then allowed to evolve for another period of time $t_2 = kt_1$, the total propagator becomes

$$\begin{aligned} U(t_2, 0) &= U(t_2, t_1)\Re U(t_1, 0) \\ &= \exp(-iH_{1/2,-1/2}t_2)\Re \\ &\quad \times \exp(-iH_{m,-m}t_1), \end{aligned} \quad (8)$$

where $\Re$ represents the transformation of a single RF pulse or a series of RF pulses that transfers the $(m, -m)$ coherence into the $(1/2, -1/2)$ central transition. Therefore, the effective Hamiltonian for the total evolution period, $t_1 + t_2$, is given by

$$\begin{aligned} H_{\text{eff}} = \frac{1}{1+k}\Big(& \sum_{l=0,2} (2m+k) A_{l0}^{\text{CS}} \\ & + \sum_{l=0,2,4} \left[C_{lm}(I) + kC_{l,1/2}(I) \right] A_{l0}^{\text{Q}} \Big) \\ & \times I_z^{1/2,-1/2}. \end{aligned} \quad (9)$$

Under the sample rotation condition, A_{l0}^{CS} and A_{l0}^{Q} become time-dependent and can be written using the Wigner rotation matrices as

$$A_{l0}^{\lambda}(t) = \sum_{m'=-l}^{l} D_{m',0}^{(l)}(\Omega^{\text{SFC}}(t)) A_{lm'}^{\lambda}, \quad (10)$$

where $\lambda = \text{CS}, \text{Q}$ and $\Omega_{\text{SFC}}(t)$ symbolizes the three Euler angles of the transformation to the laboratory frame from a sample-fixed-coordinate (SFC). In general, $A_{l0}^{\lambda}(t)$ contains second- and fourth-rank Legendre polynomials for $l = 2$ and $l = 4$, respectively. As indicated in Eqs. (2) and (3), the chemical shielding term contains only the second-rank Legendre polynomial, whereas the quadrupolar term contains both the second- and fourth-rank Legendre polynomials. The presence of both A_{20}^{Q} and A_{40}^{Q} in the quadrupolar Hamiltonian is responsible for the failure of the MAS technique in averaging out the second-order quadrupolar broadening. Clearly, the effective Hamiltonian given in Eq. (9) will not contain A_{40}^{Q} terms if the following condition can be satisfied:

$$C_{4m}(I) + kC_{4,1/2}(I) = 0 \quad \left(m = \tfrac{3}{2}, \tfrac{5}{2}, \ldots\right). \quad (11)$$

Under such a condition, the effective Hamiltonian becomes analogous to that for a chemical shielding. Therefore, MAS is sufficient to average this effective Hamiltonian, resulting in high-resolution NMR spectra. More specifically, such an effective Hamiltonian contains a time-independent part, which is the sum of the isotropic chemical shift and isotropic second-order quadrupolar shift, and a time-dependent term that contains information about the chemical shift anisotropy and second-order quadrupolar interaction. The latter time-dependent term is responsible for spinning sidebands observed in multiple-quantum NMR spectra.

2.2. *Excitation and transfer of the tripe-quantum coherence*

It is known that, for quadrupolar spin systems with $I = 3/2$, the triple-quantum $(3/2, -3/2)$ coherence can be excited by applying a weak RF pulse, i.e. $\omega_{\text{rf}} < \omega_{\text{Q}}$ [10–12]. To better understand the excitation efficiency of the triple-quantum coherence by a finite RF pulse in rotating solids, we carried out several numerical calculations. The simulations were based upon numerically evaluating the evolutions of the spin density matrix. Fig. 2a shows the excitation profile of the triple-quantum $(3/2, -3/2)$ coherence as a function of the pulse length, P_1, with different RF power levels. It is clear that in the practical range of the RF power, increased RF field strength results in a higher efficiency for the excitation of the triple-quantum coherence. For example, the excitation efficiency of the triple-quantum coherence is increased by a factor of ≈ 3 when the RF field is changed from 60 to 120 kHz. The triple-quantum excitation efficiency also depends on the strength of the quadrupolar interaction. As seen in Fig. 2b, the efficiency for the excitation of the triple-quantum $(3/2, -3/2)$ coherence is decreased as the quadrupole coupling constant increases. However, it should be noted that the triple-quantum excitation efficiency decreases to zero at two extremes: (1) $\omega_{\text{Q}} = 0$ and (2) $\omega_{\text{rf}} \ll \omega_{\text{Q}}$.

In triple-quantum experiments it is necessary to transfer the triple-quantum coherence into the central $(1/2, -1/2)$ transition. Therefore, the final sensitivity of the experiment depends not only on the triple-quantum excitation but also on the transfer

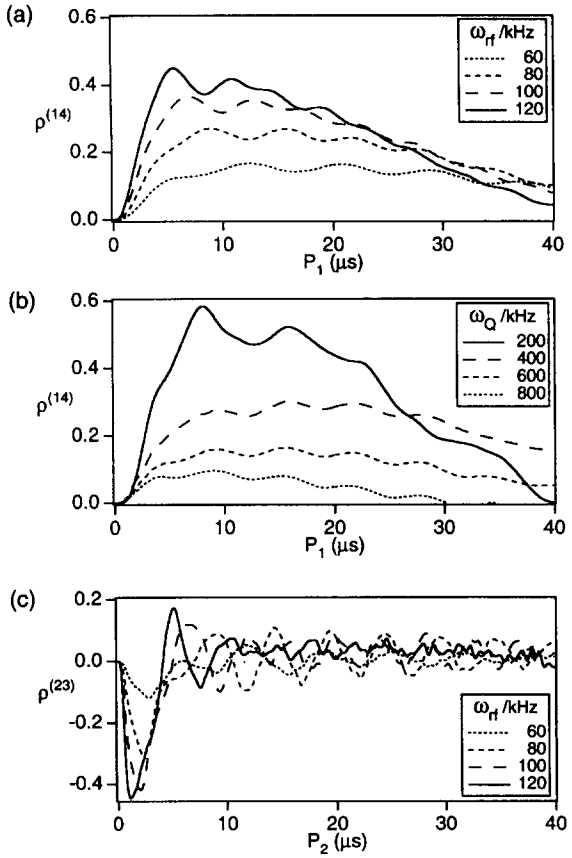

Fig. 2. (a) Calculated excitation efficiency of the triple-quantum (3/2, −3/2) coherences for $I = 3/2$ nuclei as a function of the pulse length, P_1. The quadrupole parameters used are $\omega_Q/2\pi =$ 433 kHz and $\eta = 0.6$. (b) Calculated excitation efficiency of the triple-quantum (3/2, −3/2) coherence for $I = 3/2$ nuclei as a function of the pulse length, P_1. Parameters used in the calculation are $\omega_{rf}/2\pi = 80$ kHz and $\eta = 0$. (c) Calculated transfer efficiency of the triple-quantum (3/2, −3/2) coherence to the central (1/2, −1/2) transition as a function of the pulse length, P_2. In all calculations, the sample spinning frequency was 8 kHz.

efficiency. Fig. 2c shows the calculated transfer profile in the two-pulse experiment as a function of the pulse length, P_2, with different RF field strengths. Again, the transfer efficiency increases as the RF field is increased. Interestingly, it seems that a 'solid' 180° pulse of P_2 (180° pulse for the central transition) [10,11] always gives maximum transfer efficiency. As seen in Fig. 2c, the overall signal intensity of the two-pulse sequence described here can be as high as 40% of that arising from the central transition excited by a 'solid' 90° pulse. Our simulations also indicate that the triple-quantum excitation efficiency of the two-pulse sequence is an order of magnitude larger than that of the three-pulse sequence [9].

3. Experimental

All solid-state NMR spectra were obtained on a home-built spectrometer operating at 105.22 and 53.94 MHz for ^{23}Na and ^{17}O nuclei, respectively. The MAS probe was home built and equipped with a 5 mm spinner assembly (Doty Scientific, Inc., Columbia, SC). In all ^{23}Na NMR experiments, the RF field strength was 80 kHz, corresponding to ^{23}Na 90° pulse length of 3.1 μs. The standard phase cycling scheme for selectively detecting triple-quantum coherence was used [17]. A sample of solid sodium bromide was used to accurately set the magic angle (using ^{79}Br NMR signals) and to calibrate the RF field strength at ^{23}Na NMR frequency. Anhydrous samples of Na_2SO_4 and Na_2HPO_4 were obtained from Mallinckrodt, Inc., and used without additional purification. In ^{17}O experiments, the RF field strength was 66 kHz. A liquid sample of H_2O (15% ^{17}O) was used for external referencing. All numerical simulations were performed on Digital AXP workstations using the NMRLAB program package [18].

4. Results and discussion

Fig. 3a shows the free-induction-decay (FID) signal obtained in the conventional one-pulse MAS experiment for anhydrous Na_2SO_4, which decays to zero within 500 μs. Fig. 3b displays the echo signal detected after the second pulse in the 3Q experiment with $t_1 = 1.285$ ms and $t_2 = 1.000$ ms. Fig. 3c shows the echo maxima as a function of the total evolution time, $t_1 + t_2$. In contrast to the case in Fig. 3a, the evolution of the echo lasts as long as 8 ms, indicating high resolution in the frequency domain. Indeed, the 1D 3Q-MAS spectrum, which is Fourier transform of the echo evolution shown in Fig. 3c, exhibits an isotropic peak with a line width of 109 Hz. By contrast, the MAS line shape exceeds 3 kHz.

Similarly, 3Q experiments can also be applied to other half-integer quadrupolar nuclei such as $^{17}O(I = 5/2)$. The 1D ^{17}O 3Q-MAS spectrum of solid ^{17}O-enriched hydroxyapatite ($Ca_5(P^{17}O_4)_3OH$) is shown in Fig. 4, together with the static and MAS spectrum of the same sample. The line width observed in the 3Q-MAS spectrum is approximately 330 Hz, which is an order of magnitude smaller than the 5.5 kHz width observed in the MAS spectrum. Analysis of the ^{17}O MAS spectrum yielded the following parameter: $\delta_{iso} = 117$ ppm relative to H_2O, $\omega_Q/2\pi = 240$ kHz ($e^2qQ/h = 4.8$ MHz) and $\eta = 0.2$. The isotropic ^{17}O chemical shift found for hydroxyapatite is in agreement with those reported for simple inorganic phosphates [19]. The quadrupole coupling constant determined for hydroxyapatite is also consistent with the NQR result reported for solid KH_2PO_4 [20]. Interestingly, rotational sidebands are observed in the ^{17}O 3Q-MAS spectrum of hydroxyapatite shown in Fig. 4c. In 3Q-MAS experiments, since isotropic echoes appear at $t_2 = kt_1$, the apparent spinning frequency in 3Q-MAS spectra is scaled by a factor of $1 + k$ where k is 1.58 for $I = 5/2$ nuclei. It is noted that a smaller value of k, 0.78, is required for spin-3/2 nuclei [9]. Therefore, the scaling of the spinning frequency is more severe for spin-5/2 nuclei. Similar scaled rotational sidebands have also been observed in DAS spectra [16]. As indicated by Eq. (9), the isotropic line position observed in a 3Q-MAS spectrum is different from that found in the corresponding MAS spectrum. As seen in Fig. 4, the offset of the ^{17}O MAS line shape is approximately -3.4 kHz; however, the offset of the isotropic peak in the 3Q-MAS spectrum is -0.1 kHz.

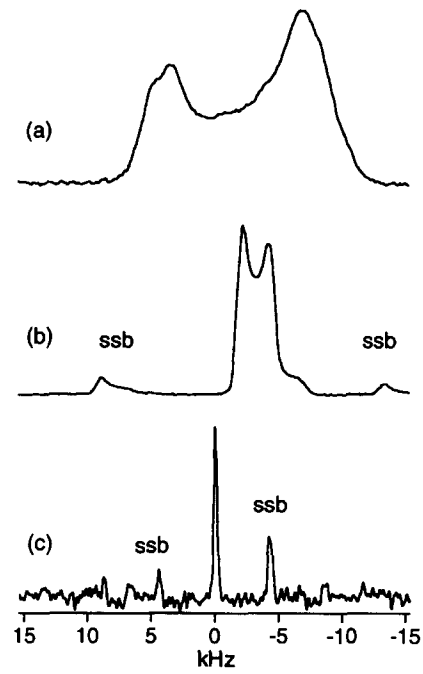

Fig. 4. ^{17}O NMR spectra of hydroxyapatite. (a) Static, (b) MAS and (c) 3Q-MAS. The sample spinning frequency used for obtaining (b) and (c) was 11.3 kHz. In (c) the t_1 increment was 12.6 μs. A total of 125 t_1 increments were collected. For each t_1 increment, a total of 624 transients were recorded. The recycle time was 1 s. The RF pulse length was 8.0 and 2.5 μs for P_1 and P_2, respectively.

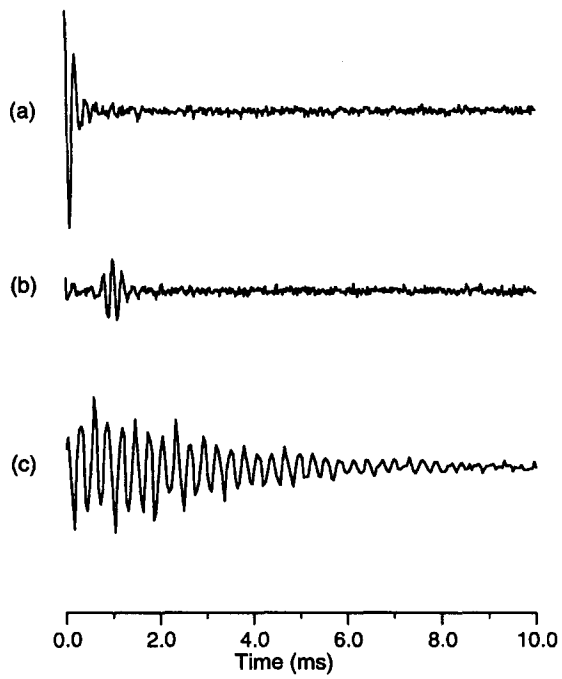

Fig. 3. (a) FID observed after one pulse under the MAS condition for anhydrous Na_2SO_4. (b) FID observed after the second pulse in the 3Q-MAS experiment with a delay between the first and second pulse being 1.285 ms. (c) Echo maximum as a function of the total evolution time, $t_1 + t_2$.

Another sample that was chosen for testing the two-pulse sequence is anhydrous Na_2HPO_4, since this sample is known to contain three crystallographically distinct Na sites with different chemical shifts and quadrupole coupling constants [21]. As discussed

earlier, 1D 3Q-MAS spectra preserve the isotropic chemical shift and isotropic second-order quadrupolar shift, and so should be useful in distinguishing between crystallographically non-equivalent sites. However, this is at a cost of losing the anisotropic information associated with individual sites. Analogous to DAS experiments [5], 3Q-MAS spectra can also be obtained in a two-dimensional (2D) fashion. If the t_2 acquisition begins at the top of echo, the resultant 2D FT spectrum will display isotropic peaks along the ω_1 dimension and their corresponding anisotropic MAS line shapes along the ω_2 dimension. The 2D ^{23}Na 3Q-MAS spectrum of anhydrous Na_2HPO_4 is shown in Fig. 5. Along the ω_1 dimension, the three crystallographically non-equivalent Na sites, Na(1), Na(2), and Na(3), are clearly observed. The line width of the three peaks is approximately 280 Hz, which is significantly narrower than the width of the corresponding MAS line shape, 8.3 kHz. The quadrupole coupling constant ($\omega_Q/2\pi$) and asymmetry parameter (η) for the three Na sites in anhydrous Na_2HPO_4 were previously reported [21]: Na(1), 355 kHz, 0.69; Na(2), 229 kHz, 0.21; Na(3), 617 kHz, 0.27. The fact that there are three crystallographically non-equivalent Na sites in anhydrous Na_2HPO_4 makes the analysis of MAS spectra difficult. In the 2D 3Q-MAS spectrum, however, all three Na sites are clearly resolved. Furthermore, slice spectra can be displayed along the ω_2 dimension from each of the isotropic positions. These slice spectra correspond to individual sub-spectra in the total MAS line shape and can be analyzed separately, yielding quadrupole parameters for each of the individual sites.

Since the positions of individual peaks in 3Q-MAS spectra are different from those in MAS, DAS or DOR spectra, caution must be exercised in interpreting 1D 3Q-MAS spectra. For example, the Na(3) site appears at the lowest frequency in the MAS and DOR spectra of anhydrous Na_2HPO_4, but it is at the

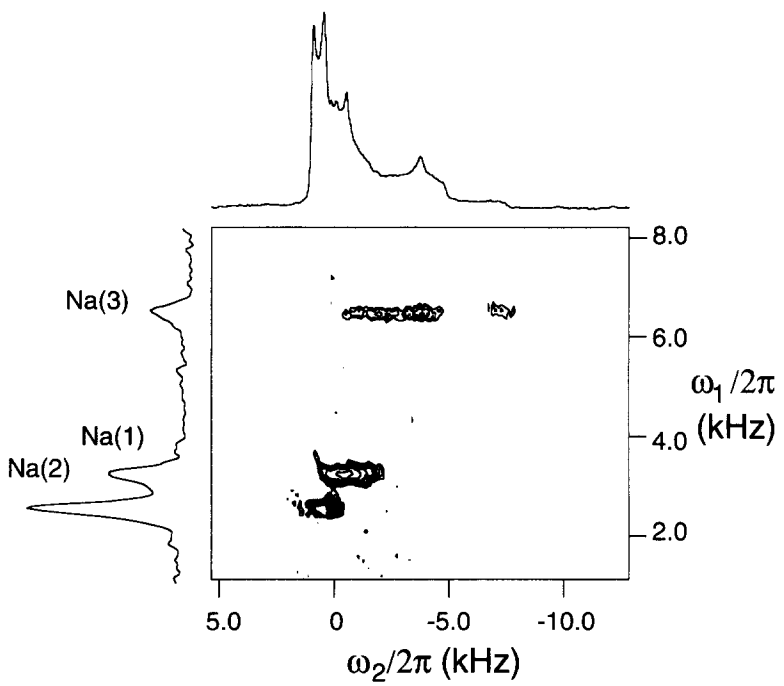

Fig. 5. 2D ^{23}Na 3Q-MAS spectrum of anhydrous Na_2HPO_4. The sample spinning frequency was 11.7 kHz. The t_1 increment was 25.7 μs. A total of 140 t_1 increments were collected. For each t_1 increment, a total of 112 transients were recorded. The recycle time was 2 s. The RF pulse length was 8.0 and 2.5 μs for P_1 and P_2, respectively. The ^{23}Na MAS spectrum (top) and 1D 3Q-MAS spectrum (left) are also shown.

highest frequency in the 1D 3Q-MAS spectrum (see Fig. 5). For $I = 3/2$ nuclei, the position of the isotropic peak in a 3Q-MAS spectrum is given by

$$\omega_{\mathrm{iso}}^{3Q} = \frac{3+k}{1+k}\omega_{\mathrm{iso}} + \frac{9}{10}\left(\frac{3-k}{1+k}\right)\frac{\omega_Q^2}{\omega_0}\left(1+\tfrac{1}{3}\eta^2\right). \quad (12)$$

Interestingly, the spacing between the three isotropic peaks in the ^{23}Na 3Q-MAS spectrum of Na_2HPO_4 is greater than the difference between the centers of the MAS line shapes for individual sites. This indicates that 3Q-MAS spectra for spin-3/2 nuclei exhibit a higher resolution than do DAS and DOR spectra. For spin-5/2 nuclei, the shift difference between isotropic peaks in triple-quantum 3Q-MAS spectra is smaller than that between the centers of individual MAS line shapes, resulting in a poor resolution compared to DAS and DOR spectra. However, quintuple-quantum (5Q) MAS spectra for spin-5/2 nuclei still exhibit a higher resolution than DAS and DOR spectra have.

It is worth noting that only one site, Na(2), was previously observed in the ^{23}Na 3Q-MAS spectrum of anhydrous Na_2HPO_4 obtained with the three-pulse sequence [9]. This suggests that the two-pulse sequence described here provides a more uniform triple-quantum excitation, which is important for detecting crystallographically non-equivalent sites. Of course, the current 3Q-MAS experiment cannot be used as a quantitative analysis. It is necessary to develop new techniques for uniform multiple-quantum excitation.

5. Conclusions

The introduction of the MQ experiment described here or the three-pulse version by Frydman and Harwood [9] is an important step towards the general goal of obtaining isotropic NMR spectra from quadrupolar nuclei which constitute a large fraction of the periodic table. Here we demonstrate the utility of the two-pulse sequence in performing 3Q-MAS experiments. Its advantage over the three-pulse sequence is twofold. First, the two-pulse sequence has a higher efficiency in generating required multiple-quantum coherences. Second, the multiple-quantum coherence excitation in the two-pulse sequence is less sensitive to the magnitude of quadrupolar interactions, making it more likely to detect all crystallographically non-equivalent sites that may have different quadrupole coupling constants. The 3Q-MAS experiment can be interpreted in either one- or two-dimensional fashion. While 1D 3Q-MAS experiments yield high-resolution isotropic spectra, the 2D presentation provides useful correlations between isotropic and anisotropic interactions.

Note added

After the submission of this paper, we learned that other research groups had also proposed the two-pulse sequence in obtaining isotropic NMR spectra for half-integer quadrupolar nuclei [22,23].

Acknowledgement

This research was supported by grants from the National Institute of Health (GM-25505 and RR-00995). GW wishes to thank the Natural Sciences and Engineering Research Council (NSERC) of Canada for a postdoctoral fellowship. We also thank Professor L. Frydman for making preprint of Ref. [9] available to us and Professor J. Virlet for helpful discussions.

References

[1] E. Kundla, A. Samonson and E. Lippmaa, Chem. Phys. Letters 83 (1981) 229.
[2] M.D. Meadows, K.A. Smith, R.A. Kinsey, T.M. Rothgeb, R.P. Skarjune and E. Oldfield, Proc. Natl. Acad. Sci. US 79 (1982) 1351.
[3] S. Ganapathy, S. Schramm and E. Oldfield, J. Chem. Phys. 77 (1982) 4360.
[4] A. Llor and J. Virlet, Chem. Phys. Letters 152 (1988) 470.
[5] K.T. Meuller, B.Q. Sun, G.C. Chingas, J.W. Zwanziger, T. Terao and A. Pines, J. Magn. Reson. 86 (1990) 470.
[6] A. Samoson, E. Lippmaa and A. Pines, Mol. Phys. 65 (1988) 1013.
[7] B.F. Chmelka, K.T. Mueller, A. Pines, J. Stebbins, Y. Wu and J.W. Zwanziger, Nature 339 (1989) 42.
[8] Y. Wu, B.Q. Sun, A. Pines, A. Samoson and E. Lippmaa, J. Magn. Reson. 89 (1990) 296.

[9] L. Frydman and J.S. Harwood, J. Am. Chem. Soc. 117 (1995) 5367.
[10] A. Wokaun and R.R. Ernst, J. Chem. Phys. 67 (1977) 1752.
[11] S. Vega, J. Chem. Phys. 68 (1978) 5518.
[12] S. Vega and Y. Naor, J. Chem. Phys. 75 (1981) 75.
[13] N.C. Nielsen, H. Bildson and H.J. Jakobsen, Chem. Phys. Letters 191 (1992) 205.
[14] N.C. Nielsen, H. Bildson and H.J. Jakobsen, J. Magn. Reson. 97 (1992) 149.
[15] J. Virlet, private communication.
[16] B.Q. Sun, J.H. Baltisberger, Y. Wu, A. Samoson and A. Pines, Solid State Nucl. Magn. Reson. 1 (1992) 267.
[17] A. Wokaun and R.R. Ernst, Chem. Phys. Letters 52 (1977) 407.
[18] B.Q. Sun and R.G. Griffin, to be published.
[19] J.A. Gerlt, P.C. Demou and S. Mehdi, J. Am. Chem. Soc 104 (1982) 2848.
[20] R. Blinc, J. Seliger, R. Osredkar and M. Mali, Phys. Letters 47a (1974) 131.
[21] M. Baldus, B.H. Meier, R.R. Ernst, A.P.M. Kentgens, H. Meyer zu Altenschildesche and R. Nesper, J. Am. Chem. Soc. 117 (1995) 5141.
[22] C. Fernandez and J.P. Amoureux, Chem. Phys. Letters 242 (1995) 449; Solid State Nucl. Magn. Reson., in press.
[23] A. Medek, J.S. Harwood and L. Frydman, J. Am. Chem. Soc., in press.